

arXiv:gr-qc/9807060v1 22 Jul 1998

Non-singular Bianchi type I cosmological solutions from 1-loop superstring effective action

Shinsuke KAWAI*

Graduate School of Human and Environmental Studies, Kyoto University, Kyoto 606-8501, Japan

Jiro SODA†

Department of Fundamental Sciences, FIHS, Kyoto University, Kyoto 606-8501, Japan

(December 2, 2024)

Non-singular Bianchi type I solutions are found from the effective action with a superstring-motivated Gauss-Bonnet term. These anisotropic non-singular solutions evolve from the asymptotic Minkowski region, subsequently super-inflate, and then smoothly continue either to Kasner-type (expanding in two directions and shrinking in one direction) or to Friedmann-type (expanding in all directions) solutions. We also found a new kind of singularity which arises from the fact that the anisotropic expansion rates are multiple-valued function of time. The initial singularity in the isotropic limit of this model belongs to this new kind of singularity. In our analysis the anisotropic solutions are likely to be singular when the super-inflation is steep.

*E-mail:kawai@phys.h.kyoto-u.ac.jp

†E-mail:jiro@phys.h.kyoto-u.ac.jp

I. INTRODUCTION

Stimulated by the developments of the superstring theory, various cosmological solutions based on the string theory have been proposed by now. Although the theory has not developed enough to present the unique history of our universe in its earliest stage, one may now imagine that the big bang is no longer just a point of enigma named initial singularity but it has a rich and complex structure.

Among these string-based universe models, the most widely studied one would be the so-called pre-big-bang model [1] (in the literature it is often called string cosmology). The remarkable aspect of this model is that it tries to explain the inflationary behavior of the early universe by introducing the pole-like acceleration phase (super-inflation) which is driven by the kinetic term of the dilaton. This super-inflationary branch of the solution has a dual relation named scale factor duality with the Friedmann branch, which is the usual decelerating expansion of the universe. The biggest problem arising in the pre-big-bang model is the difficulty of connecting the super-inflationary branch and the Friedmann branch (termed graceful exit problem), and there are no-go theorems proven under some assumptions [2].

Antoniadis, Rizos and Tamvakis [3] proposed a non-singular (i.e. free of graceful exit problem) cosmological model by including the 1-loop (genus) correction term in the low-energy string effective action. Although it might be less motivated compared with pre-big-bang, this 1-loop model is excellent in that it gives a simple example of smooth transition between super-inflationary branch and the Friedmann branch. This original 1-loop model involves dilaton and modulus fields, and there is a simplified version [4] by Rizos and Tamvakis with modulus field only. This metric-modulus system gives essentially the same non-singular solution as the full metric-dilaton-modulus system, since the behavior of the solution mainly depends only on the modulus field. The existence of the non-singular solution is analytically shown by Rizos and Tamvakis [4] for the FRW metric, i.e. assuming the homogeneity and isotropy of the universe. We studied whether the nature of this non-singular solution is affected if anisotropy is included. The purpose of this paper is to extend the solution of this metric-modulus system to include anisotropy, and to observe the behavior of its solutions, particularly of non-singular ones.

The following sections of this paper are organized as follows. In the section II we briefly review the isotropic case studied by Rizos and Tamvakis [4], and then derive the basic equations of motion from the effective action for Bianchi type I metric. We also solve these equations analytically in the asymptotic region. In section III we solve these equations numerically. We study the solutions through several cross sections of the parameter space. The existence of non-singular anisotropic solutions are shown, and the nature of the singularity is also

examined. Implications of our results are discussed in the last section.

II. MODEL AND EQUATIONS OF MOTION

We start with the action given by [4]:

$$\mathcal{S} = \int d^4x \sqrt{-g} \left\{ \frac{1}{2}R - \frac{1}{2}(D\sigma)^2 - \frac{\lambda}{16}\xi(\sigma)R_{GB}^2 \right\}, \quad (1)$$

which is essentially the same as the 1-loop corrected 4-dimensional effective action of orbifold-compactified heterotic string [3]:

$$\mathcal{S} = \int d^4x \sqrt{-g} \left\{ \frac{1}{2}R - \frac{1}{4}(D\Phi)^2 - \frac{3}{4}(D\sigma)^2 + \frac{1}{16}[\lambda_1 e^\Phi - \lambda_2 \xi(\sigma)]R_{GB}^2 \right\} \quad (2)$$

except that the dilaton field σ is neglected. R , Φ and σ are the Ricci scalar curvature, the dilaton, and the modulus field, respectively. Our convention is $g_{\mu\nu} = (-, +, +, +)$, $R^\mu_{\alpha\nu\beta} = \Gamma^\mu_{\alpha\beta,\nu} + \dots$, $R_{\alpha\beta} = R^\mu_{\alpha\mu\beta}$ and $8\pi G = 1$. The Gauss-Bonnet curvature is defined as $R_{GB}^2 = R^{\mu\nu\kappa\lambda}R_{\mu\nu\kappa\lambda} - 4R^{\mu\nu}R_{\mu\nu} + R^2$, and $\xi(\sigma)$ is a function determining the coupling of σ and the geometry, written in terms of the Dedekind η function as

$$\begin{aligned} \xi(\sigma) &= -\ln[2e^\sigma\eta^4(ie^\sigma)] \\ &= -\ln 2 - \sigma + \frac{\pi e^\sigma}{3} - 4 \sum_{n=1}^{\infty} \ln(1 - e^{-2n\pi e^\sigma}). \end{aligned} \quad (3)$$

This $\xi(\sigma)$, an even function of σ , has a global minimum at $\sigma = 0$ and increases exponentially as $\sigma \rightarrow \pm\infty$. λ_1 is the four-dimensional string coupling and takes a positive value. λ_2 is proportional to four-dimensional trace anomaly of the $N=2$ sector and determined by the number of chiral, vector and spin- $\frac{3}{2}$ supermultiplets. It is important that λ_2 can take positive values, since non-singular solutions arise only when $\lambda_2 > 0$. In our simplified model(1), therefore, we assume λ to be positive (in actual numerical calculations we set $\lambda = 1$) and adopt the form of the ξ function (3).

A. ISOTROPIC SOLUTIONS

Firstly, we consider the homogeneous and isotropic case which is discussed in [4]. We neglect the spatial curvature and write the metric in the flat FRW form:

$$ds^2 = -N(t)^2dt^2 + a(t)^2(dx^2 + dy^2 + dz^2). \quad (4)$$

Variation of the action(1) with respect to the lapse N , the scale factor a , and the modulus field σ gives three equations of motion as

$$\ddot{\sigma}^2 = 6H^2(1 - \frac{\lambda}{2}H\dot{\xi}) \quad (5)$$

$$(2\dot{H} + 5H^2)(1 - \frac{\lambda}{2}H\dot{\xi}) + H^2(1 - \frac{\lambda}{2}\ddot{\xi}) = 0 \quad (6)$$

$$\ddot{\sigma} + 3H\dot{\sigma} + \frac{3\lambda}{2}(\dot{H} + H^2)H^2\frac{\partial\xi}{\partial\sigma} = 0, \quad (7)$$

where H is the Hubble parameter \dot{a}/a , the dot (\cdot) means derivative with respect to physical time t and we have set $N(t) = 1$. Due to the absence of scales (we are only considering spatially flat metric (4)) and the existence of the constraint (5), the solutions are completely determined by a couple of first order differential equations for two variables H and σ , that is, if we give values of H and σ at some time t , the precedent and following evolution of the solution is automatically determined by these equations.

Fig.1 shows the H - σ phase diagram of the isotropic system solved with initial conditions $H > 0$ and $\dot{\sigma} > 0$. These solution flows are distinguished by only one degree of freedom (for example, the value of H at some fixed $\sigma > 0$). There are singular solutions and non-singular solutions, and it is shown in [4] that all flows in the $H > 0, \sigma < 0$ quarter plane continue smoothly to $H > 0, \sigma > 0$ quarter plane, but some flows in $H > 0, \sigma > 0$ quarter plane go into singularity and do not continue to $\sigma < 0$ region. It is also shown in [4] that the signs of H and $\dot{\sigma}$ are conserved throughout the evolution of the system. Since $\dot{\sigma}$ is always positive in the fig.1, time flows from left to right. We consider our Friedmann universe corresponds to the “future” region ($\sigma > 0$) in the fig.1, and we regard the “past” region ($\sigma < 0$) with increasing Hubble parameter as a super-inflation, which is expected to solve the shortcomings of the big-band model.

B. EQUATIONS OF MOTION

We now extend the above model to anisotropic Bianchi type I space-time. We write the metric as

$$ds^2 = -N(t)^2dt^2 + e^{2\alpha(t)}dx^2 + e^{2\beta(t)}dy^2 + e^{2\gamma(t)}dz^2, \quad (8)$$

and define the anisotropic expansion rates as

$$p = \dot{\alpha}, \quad q = \dot{\beta}, \quad r = \dot{\gamma}. \quad (9)$$

The average expansion rate, which becomes the Hubble parameter H in the isotropic limit, is

$$H_{\text{avr}} = \frac{1}{3}(p + q + r). \quad (10)$$

The equations of motion are obtained by variation of the action (1) with respect to N, α, β, γ and σ , viz.

$$pq + qr + rp - \frac{1}{2}\dot{\sigma}^2 - \frac{3}{2}\lambda\frac{\partial\xi}{\partial\sigma}\dot{\sigma}pqr = 0, \quad (11)$$

$$\dot{p} = \frac{(CA - EB)G + (EF - A^2)H + (AB - FC)Q}{\Delta}, \quad (12)$$

$$\dot{q} = \frac{(BC - DA)G + (BA - FC)H + (FD - B^2)Q}{\Delta}, \quad (13)$$

$$\dot{r} = \frac{(DE - C^2)G + (AC - BE)H + (BC - AD)Q}{\Delta}, \quad (14)$$

$$\ddot{\sigma} + (p + q + r)\dot{\sigma} + \frac{1}{2}\lambda\frac{\partial\xi}{\partial\sigma}\{\dot{pqr} + p\dot{qr} + p\dot{qr} + pqr(p + q + r)\} = 0, \quad (15)$$

where

$$A = 1 - \frac{\lambda}{2}\frac{\partial\xi}{\partial\sigma}\dot{\sigma}p + \frac{\lambda^2}{4}(\frac{\partial\xi}{\partial\sigma})^2p^2qr, \quad (16)$$

$$B = 1 - \frac{\lambda}{2}\frac{\partial\xi}{\partial\sigma}\dot{\sigma}q + \frac{\lambda^2}{4}(\frac{\partial\xi}{\partial\sigma})^2pq^2r, \quad (17)$$

$$C = 1 - \frac{\lambda}{2}\frac{\partial\xi}{\partial\sigma}\dot{\sigma}r + \frac{\lambda^2}{4}(\frac{\partial\xi}{\partial\sigma})^2pqr^2, \quad (18)$$

$$D = \frac{\lambda^2}{4}(\frac{\partial\xi}{\partial\sigma})^2q^2r^2, \quad (19)$$

$$E = \frac{\lambda^2}{4}(\frac{\partial\xi}{\partial\sigma})^2r^2p^2, \quad (20)$$

$$F = \frac{\lambda^2}{4}(\frac{\partial\xi}{\partial\sigma})^2p^2q^2, \quad (21)$$

$$G = -p^2 - q^2 - qr - \frac{1}{2}\dot{\sigma}^2 + \frac{\lambda}{2}\frac{\partial^2\xi}{\partial\sigma^2}\dot{\sigma}^2pq - \frac{\lambda}{2}\frac{\partial\xi}{\partial\sigma}\dot{\sigma}pqr - \frac{\lambda}{4}(\frac{\partial\xi}{\partial\sigma})^2p^2q^2r(p + q + r), \quad (22)$$

$$H = -q^2 - r^2 - qr - \frac{1}{2}\dot{\sigma}^2 + \frac{\lambda}{2}\frac{\partial^2\xi}{\partial\sigma^2}\dot{\sigma}^2qr - \frac{\lambda}{2}\frac{\partial\xi}{\partial\sigma}\dot{\sigma}pqr - \frac{\lambda}{4}(\frac{\partial\xi}{\partial\sigma})^2pq^2r^2(p + q + r), \quad (23)$$

$$Q = -r^2 - p^2 - rp - \frac{1}{2}\dot{\sigma}^2 + \frac{\lambda}{2}\frac{\partial^2\xi}{\partial\sigma^2}\dot{\sigma}^2rp - \frac{\lambda}{2}\frac{\partial\xi}{\partial\sigma}\dot{\sigma}pqr - \frac{\lambda}{4}(\frac{\partial\xi}{\partial\sigma})^2p^2qr^2(p + q + r), \quad (24)$$

and

$$\Delta = 2ABC + DEF - FC^2 - DA^2 - EB^2. \quad (25)$$

In the isotropic limit, equations (11) and (15) become (5) and (7) respectively, and (12) (13)(14) reduce to one equation (6). As is similar to the isotropic case, once the values of σ, p, q and r are given at some time t and $\dot{\sigma}$ is given according to the constraint (11), the system evolves along the flow of the solution following the equations (12)~(15). There are five parameters($\sigma, \dot{\sigma}, p, q$, and r) and one constraint (11), so the solution flows are drawn in a 4-dimensional space, for example, σ - p - q - r space. Since the aim of this paper is to examine the effect of anisotropy to the non-singular solution, we observe the change of the solution as we increase the anisotropy of the metric. To facilitate this we introduce two parameters indicating the anisotropy of the metric, viz.

$$X = \frac{p-r}{p+q+r}, \quad Y = \frac{q-r}{p+q+r}. \quad (26)$$

In this notation, $(X, Y) = (0, 0)$ corresponds to the isotropic(FRW) metric, and postulating H_{avr} to be positive, the region surrounded by the lines $Y = 2X + 1$, $Y = \frac{1}{2}X - \frac{1}{2}$, $Y = -X + 1$ indicates the universe expanding in all directions (These lines are drawn in the figs.3 and 6). The regions $Y < 2X + 1$, $Y > \frac{1}{2}X - \frac{1}{2}$, $Y > -X + 1$ etc. are the “Kasner-like” universe expanding in two directions and contracting in one direction. The regions $Y > 2X + 1$, $Y > \frac{1}{2}X - \frac{1}{2}$, $Y > -X + 1$ etc. describes the universe expanding in one direction, contracting in two directions. The universe shrinking in all directions can not be included if we use (26) and assume $H_{\text{avr}} > 0$. Instead of σ - p - q - r we use σ - H_{avr} - X - Y as four variables describing our system.

C. ASYMPTOTIC SOLUTIONS

Before going to the numerical analysis, we study the asymptotic form of the solutions at $t \rightarrow \pm\infty$, $|\sigma| \rightarrow \infty$. We assume σ to become large when $t \rightarrow \pm\infty$. The asymptotic form of the derivatives of the function ξ are

$$\frac{\partial \xi}{\partial \sigma} \sim \text{sign}(\sigma) \frac{\pi}{3} e^{|\sigma|}, \quad (27)$$

$$\frac{\partial^2 \xi}{\partial \sigma^2} \sim \frac{\pi}{3} e^{|\sigma|}. \quad (28)$$

If we assume the power-law ansatz for the expansion rates, the asymptotic form of the modulus has to be logarithmic in order to cancel the exponential dependence of (27) and (28). Thus we choose the following forms for the asymptotic solutions:

$$p \sim \omega_1 |t|^\rho, \quad (29)$$

$$q \sim \omega_2 |t|^\rho, \quad (30)$$

$$r \sim \omega_3 |t|^\rho, \quad (31)$$

$$\sigma \sim \sigma_0 + \omega_4 \ln |t|. \quad (32)$$

Putting all these into equations (11)~(15), we obtain two possible asymptotic solutions:

$$\mathcal{A} : \rho = -1, \omega_1 + \omega_2 + \omega_3 = \text{sign}(t), \\ \omega_1^2 + \omega_2^2 + \omega_3^2 + \omega_4^2 = 1. \quad (33)$$

$$\mathcal{B} : \rho = -2, |\omega_4| = 5, \\ \omega_1 \omega_2 \omega_3 = -\text{sign}(t) \frac{5 \exp[-\sigma_0 \text{sign}(\omega_4)]}{\lambda \pi}. \quad (34)$$

The solution \mathcal{A} is obtained by balancing the terms that do not include 1-loop effect, i.e. the Gauss-Bonnet term, and thus describes the asymptotic behavior where the Gauss-Bonnet effect is negligible. In the absence of the modulus field, \mathcal{A} is nothing but the Bianchi type I vacuum (Kasner) solution. The solution \mathcal{B} is obtained by balancing the kinetic term of the modulus and the Gauss-Bonnet

term, and this solution corresponds to the phase where the Gauss-Bonnet term is important. Other possibilities of solutions are excluded as long as we impose $\lambda > 0$, which is, in the isotropic limit, a necessary condition for the existence of the non-singular solutions.

Following the isotropic case [3] [4] [5], we choose $\dot{\sigma} > 0$ and assume the solution \mathcal{A} in the future asymptotic region and \mathcal{B} in the past asymptotic region. Then in the region $t \rightarrow \infty$, the conditions (33) can be seen in the ω_1 - ω_2 - ω_3 space as the cross section of the sphere of radius $\sqrt{1 - \omega_4^2}$ centered at the origin with the $\omega_1 + \omega_2 + \omega_3 = 1$ plane. Depending the asymptotic value of ω_4 , the asymptotic solutions of $t \rightarrow \infty$ are categorized into two cases

$\mathcal{A}1)$ $0 \leq \omega_4 < \sqrt{\frac{1}{2}}$: The asymptotic solution is either expanding in all directions (Friedmann type) or expanding in two directions, shrinking in one direction (Kasner-type).

$\mathcal{A}2)$ $\sqrt{\frac{1}{2}} \leq \omega_4 \leq \sqrt{\frac{2}{3}}$: The asymptotic solution is Friedmann type only.

In terms of X and Y introduced in (26), the asymptotic solution is represented by a point on a arc of the ellipse $X^2 + Y^2 - XY = 1 - \frac{3}{2}\omega_4^2$. Thus $\mathcal{A}2)$ falls onto the region inside the oval $X^2 + Y^2 - XY = \frac{1}{4}$, and $\mathcal{A}1)$ is in the region between two ellipses $X^2 + Y^2 - XY = \frac{1}{4}$ and $X^2 + Y^2 - XY = 1$. No asymptotic solutions exist in the region outside the ellipse $X^2 + Y^2 - XY = 1$, where the constraint equation (11) is not satisfied. Therefore, at least in the far enough future region, it is sufficient to examine the solutions near the isotropic one. The difference of our model from the Kasner (Bianchi type I vacuum) solution is the existence of the field σ , which allows the existence of Friedmann-type solution in the future asymptotic region.

In the past asymptotic region, the condition (34) indicates $\omega_1 \omega_2 \omega_3 > 0$, i.e.

$\mathcal{B}1)$ $\omega_1, \omega_2, \omega_3 > 0$, or

$\mathcal{B}2)$ One of ω_i ($i = 1, 2, 3$) is positive, two are negative. This means in the past asymptotic region the universe is either expanding in all directions, or expanding in one direction, contracting in two directions.

III. NUMERICAL RESULTS

Once the anisotropy is included, the behavior of the solution deviates substantially from the isotropic case. Fig.2 shows the average expansion rate $H_{\text{avr}} = (p + q + r)/3$ versus the modulus σ in the anisotropic (Bianchi type I) case, solved with initial anisotropy $X = 0.1$, $Y = 0.2$ at $\sigma = -10$. Unlike the isotropic case (fig.1), some solution flows in the $\sigma < 0$ region do not continue smoothly to $\sigma > 0$ region, but terminate suddenly with finite values of σ and H_{avr} . At these queer singularities the time derivatives of p , q and r become infinite, although p , q and r themselves stay finite. This is because the value of Δ (25) approaches zero, while the numera-

tors of the equations (12), (13) and (14) stay finite. Thus, the function Δ plays an important role in the anisotropic case, and the regularity of the solutions depends largely on its behavior.

In the equations in our model there are four independent variables, σ - H_{avr} - X - Y . Since our interest is mainly in the vicinity of the isotropic solution, we examine the solutions which pass near the origin of the X - Y plane, first at $\sigma = -10$ section with several different values of H_{avr} , and next at $\sigma = 2.5$ section.

A. SOLUTIONS THROUGH $\sigma = -10$ CROSS SECTION

It is helpful to consider the general behavior of Δ and the region prohibited by the constraint equation before solving the equations numerically. Rewriting Δ (25) and the constraint equation (11) in terms of σ , H_{avr} , X and Y , we can specify $\Delta > 0$, $\Delta < 0$ and prohibited regions on X - Y plane for fixed σ and H_{avr} , which is shown in the fig.3. The dark-shaded region is the prohibited region, the light-shaded region is where $\Delta < 0$, and the white region is where $\Delta > 0$. Since $\Delta = 0$ is not physically allowed (\dot{p} , \dot{q} and \dot{r} diverge from (12), (13) and (14)), the solutions in the white region cannot go smoothly to the light-shaded region. Also indicated in the fig.3 is the lines $X + Y = 1$, etc. discussed in the subsection B of the section II. We can see that the universe expanding in all directions always lie in $\Delta > 0$ region. For larger H_{avr} the prohibited region becomes thinner, and the white and light gray regions will be separated by the lines $X + Y = 1$, etc.

Starting from the initial conditions $\sigma = -10$ and $H_{\text{avr}} = 0.001, 0.005, 0.01$, we solved the equations future-ward and indicated the behavior of the solutions in the X - Y plane (fig.4). Because of the symmetry of the axes, we restrict the region to $X > 0$, $Y > 0$, and since we are not interested in the prohibited region we only examined the vicinity of the origin.

The black region in the fig.4 is prohibited by the hamiltonian constraint, and the regions marked NS means non-singular solutions. The difference between NSa and NSb is in their form in the future asymptotic region, where NSa has Friedmann-type (expanding in all directions) and NSb has Kasner-type (expanding in two directions and contracting in one direction) asymptotic solutions. Examples of NSa and NSb solutions are shown in the first and the second panels of the fig.5. The solutions in the region marked S1 in the fig.4 lead to singularities where $\Delta \rightarrow 0$, (we term this singularity type I) and these singular solutions are the same as those appeared in the fig.2. We divided the S1 solutions into two classes, S1a and S1b. S1a approaches the singularity as $p\dot{p} > 0$, $q\dot{q} > 0$, $r\dot{r} > 0$, while S1b as $p\dot{p} < 0$, $q\dot{q} < 0$, $r\dot{r} < 0$. This singularity, since it arises because Δ crosses zero, can be overpassed if we introduce a new “time” variable,

$$d\tau = \Delta dt. \quad (35)$$

Using this τ , two solutions S1a and S1b can be joined via the singularity, which is shown in the third panel of the fig.5 (S1a,b). The solution S1b, solved backwards in time, goes into another singularity which has different property from the one between S1a and S1b. At this singularity, which we call type II, Δ goes to $-\infty$, and at least one of the expansion rates (q in the case of fig.5 S1a,b) diverges. We can say that this solution (S1a and S1b joined together) comes regularly from $t = -\infty$, turns back at type I singularity, and then goes backwards in time into a type II singularity. Or, we can also see this as two solutions, one coming from $t = -\infty$ and the other from type II singularity, “pair-annihilate” at one type I singularity. S2 is yet another solution, which comes from one type II singularity and disappears into another type II singularity. As H_{avr} becomes larger, the boundary between S1a and S1b ($\Delta = 0$ line in the fig.3) gets pushed to approach the line $X + Y = 1$, and accordingly the non-singular region NSa and NSb become smaller. This is consistent with the fig.2, which shows the existence of the upper limit of H_{avr} for the regular solution through $\sigma < 0$ region.

B. SOLUTIONS THROUGH $\sigma = 2.5$ CROSS SECTION

As is expected from the isotropic case discussed in the previous section, the solutions through $\sigma > 0$ cross section are quite different from those through $\sigma < 0$ section. In fig.6 we show the constrained region (dark-shaded), $\Delta > 0$ region (white) and $\Delta < 0$ region (light shaded) in the X - Y plane, with σ fixed to 2.5. The elliptic allowed region of small H_{avr} is the one discussed in relation with the future asymptotic form of the solution, which is expressed as $X^2 + Y^2 - XY = 1$. As H_{avr} takes large values the $\Delta = 0$ contour takes complicated forms, and the region connected to the isotropic solution becomes small.

Fig.7 shows the solutions passing through the X - Y plane of the $\sigma = 2.5$ cross section, and the time evolution of each type is shown in the fig.8. H_{avr} is chosen to be 0.01, 0.05 and 0.1. As H_{avr} increases the non-singular region becomes smaller, and for H_{avr} larger than 0.1 the non-singular solution completely disappears from the X - Y plane. All the singularities appearing in fig.7 are type I, and these singular solutions can be extended further by using τ defined by (35). Just like the S1a and S1b solutions in the previous subsection, S1c and S1d, extended beyond the type I singularity, turn back future-wards and then go into type II singularity. The only difference between these and S1a,b is the direction of the time, and the former can be regarded as the “pair-creation” of cosmological solutions, while the latter is the “pair-annihilation.”

One of the non-trivial results of our analysis, and what makes this model very different from the ordinary universe models, is that the “initial singularity” in the isotropic limit is categorized into the type I singularity (see the third panel of fig.7 and compare S1d and Isotropic solutions in fig.8). This means that the singular solutions in the model proposed by Antoniadis, Rizos and Tamvakis [3], or Rizos and Tamvakis [4] will, if small anisotropy is included, terminate suddenly at finite past with finite Hubble parameter, or, if extended using τ , turn back towards future.

All non-singular solutions in the fig.7 and fig.8 continue to the asymptotic solutions expanding in all directions in the past asymptotic region. That is, the asymptotic form $\mathcal{B}1$ (discussed in the subsection C of the section II) can be reached from $\sigma = 2.5$ but $\mathcal{B}2$) cannot. There exist solutions having the past asymptotic form $\mathcal{B}2$). For example, solutions through the outer white ($\Delta > 0$) region in the third panel of fig.3 behave as $\mathcal{B}2$) in the $t \rightarrow -\infty$ region. These solutions, however, go into singularities between $\sigma = -10$ and $\sigma = 2.5$, and do not appear in the fig.7 or fig.8.

C. SUMMARY OF NUMERICAL RESULTS

We extended the non-singular universe model proposed by Rizos and Tamvakis [4] to include anisotropy, and examined the solutions in the vicinity of isotropic solution in both $\sigma < 0$ and $\sigma > 0$ regions. We found both non-singular solutions and singular solutions. Non-singular solutions inhabit in the region where the anisotropy is small, and they evolve from the past asymptotic region, super-inflate, and then lead either to Friedmann-type or to Kasner-type solutions in the future. Singularities appearing in our analysis are classified into two types, namely, type I and type II. The type I singularity corresponds to the crossing of $\Delta = 0$, and \dot{p} , \dot{q} , or \dot{r} diverge, while p , q , r , and σ , $\dot{\sigma}$ stay finite. At type II singularity, on the other hand, Δ tends to $-\infty$, and p , q or r will diverge. The evolution of the singular solutions is characterized by the behavior of Δ . At the origin of the X - Y plane (isotropic solution) Δ is always positive regardless of the values of σ or H_{avr} , and as anisotropy increases there appear $\Delta < 0$ regions, or the regions prohibited by the constraint equation(11), which is shown in the fig.3 and fig.6. There are three types of singular solutions appearing in our analysis (if two branches connected by type I singularity are counted as one solution). The first type of singular solution is marked by crossing of $\Delta = 0$ line, which we termed type I singularity, in the future. This includes S1a and S1b in the fig.4 and fig.5, and if we continue the solution beyond $\Delta = 0$ by changing the variable, this singular solution can be seen as a pair-annihilation of $\Delta > 0$ and $\Delta < 0$ branches of solutions. $\Delta > 0$ branch continues from infinite past, while $\Delta < 0$ branch leads to type II singularity at finite past.

The second singular solution is very similar to the first one, except it crosses $\Delta = 0$ line in the past. This solution, examples of which are S1c and S1d of fig.7 and fig.8, can be regarded as a pair-creation of two branches. The singular solution in the isotropic model [3,4] is a special case of this second singular solution. The third singular solution lies always in $\Delta < 0$ region and never crosses $\Delta = 0$ line, i.e. includes no type I singularity. This solution is born in the type II singularity, and disappears into type II singularity (see S2 of fig.4 and fig.5).

IV. CONCLUSION

In this paper we presented anisotropic non-singular cosmological solutions derived from the 1-loop effective action of the heterotic string. We found non-singular solutions which evolve from infinite past asymptotic region, super-inflate, and then continue either to Friedmann-type or Kasner-type solutions. The singular solutions of moderate anisotropy is classified into three types, and involved in these solutions are two types of singularities, one corresponds to $\Delta = 0$ and the other to $\Delta = -\infty$. The initial singularity in the isotropic limit is a special case of $\Delta = 0$ singularity.

The violation of the energy conditions, which is necessary to avoid the singularity, is achieved by the existence of the Gauss-Bonnet term coupled to modulus field. This can be confirmed by using the asymptotic forms(33) and (34) for non-singular solutions. We define the effective energy density and effective pressure as

$$\epsilon := -G^0_0 = pq + qr + rp, \quad (36)$$

$$p_1 := G^1_1 = -(\dot{q} + \dot{r} + q^2 + r^2 + qr), \quad (37)$$

$$p_2 := G^2_2 = -(\dot{r} + \dot{p} + r^2 + p^2 + rp), \quad (38)$$

$$p_3 := G^3_3 = -(\dot{p} + \dot{q} + p^2 + q^2 + pq). \quad (39)$$

Assuming the asymptotic solution \mathcal{A} in the region $t \rightarrow \infty$ and that $\dot{\sigma}$ is always positive (in our numerical analysis $\dot{\sigma}$ keeps its sign except the singular solution S2), the effective energy density and pressure behave in the future asymptotic region as $\epsilon, p_i \sim \frac{1}{2}\omega_4^2|t|^{-2}$ ($i = 1, 2, 3$). Thus, the weak energy condition $\epsilon + p_i \sim \omega_4^2|t|^{-2} > 0$ and the strong energy condition $\epsilon + \sum p_i \sim 2\omega_4^2|t|^{-2} > 0$ are satisfied. In the past asymptotic region, on the other hand, the asymptotic solution becomes \mathcal{B} in which the Gauss-Bonnet term is dominant. Then $\epsilon \sim (\omega_1\omega_2 + \omega_2\omega_3 + \omega_3\omega_1)|t|^{-4}$ and $p_1 \sim -2(\omega_2 + \omega_3)|t|^{-3} - (\omega_2^2 + \omega_3^2 + \omega_2\omega_3)|t|^{-4}$, etc. If the weak energy condition is satisfied, $\epsilon + p_i > 0$ for $i = 1, 2, 3$ so $3\epsilon + \sum p_i \sim -4(\omega_1 + \omega_2 + \omega_3)|t|^{-3}$ must be positive. If the strong energy condition is satisfied, $\epsilon + \sum p_i \sim -4(\omega_1 + \omega_2 + \omega_3)|t|^{-3}$ must be positive. Neither of them are possible as long as $H_{\text{avr}} \sim (\omega_1 + \omega_2 + \omega_3)|t|^{-2}/3 > 0$. Therefore, weak and strong energy conditions are violated in the past asymptotic region.

One of the largest advantages of our model is that it includes a rather long period of (super-)inflationary stage

in a natural form. However, our result, which admits the evolution of an almost-isotropic super-inflating solution into Kasner-type anisotropic solution (see the panel “NSb” of the fig.5 for example), suggests that the super-inflation in our model does not isotropize the space-time. Our recent study [6] on the cosmological perturbation for the homogeneous and isotropic background shows the existence of exponential growth in graviton-mode perturbation during the super-inflationary stage. Together with this we can conclude that the cosmic no-hair hypothesis [7] does not hold in this super-inflationary model. We are interested in whether this result is common to all kinetic-driven super-inflation.

ACKNOWLEDGMENTS

This work of J.S. is supported by the Grant-in-Aid for Scientific Research 10740118.

- [1] M. Gasperini and G. Veneziano, *Astropart. Phys.* **1**(1993) 317, *Mod. Phys. Lett.* **A8**(1993) 3701, *Phys. Rev.* **D50**(1994) 2519.
- [2] R. Brustein and G. Veneziano, *Phys. Lett.* **B329**(1994) 429; N. Kaloper, R. Madden and K. A. Olive, *Nucl. Phys.* **B452**(1995)677; M. Gasperini, M. Maggiore and G. Veneziano, *Nucl. Phys.* **B494**(1997) 315; R. Brustein and R. Madden, *hep-th/9702043*.
- [3] I. Antoniadis, J. Rizos and K. Tamvakis, *Nucl. Phys.* **B415**(1994) 497.
- [4] J. Rizos and K. Tamvakis, *Phys. Lett.* **B326**(1994) 57.
- [5] R. Easther and K. Maeda, *Phys. Rev.* **D54**(1996) 7252.
- [6] S. Kawai, M. Sakagami and J. Soda, *gr-qc/9802033*, submitted to *Phys. Lett.* **B**.
- [7] R. Wald, *Phys. Rev.* **D28**(1983) 2118, M. S. Turner and L. M. Widrow, *Phys. Rev. Lett.* **57**(1986) 2237, L. G. Jensen and J. A. Stein-Schabes, *Phys. Rev.* **D34**(1986) 931.

Figures

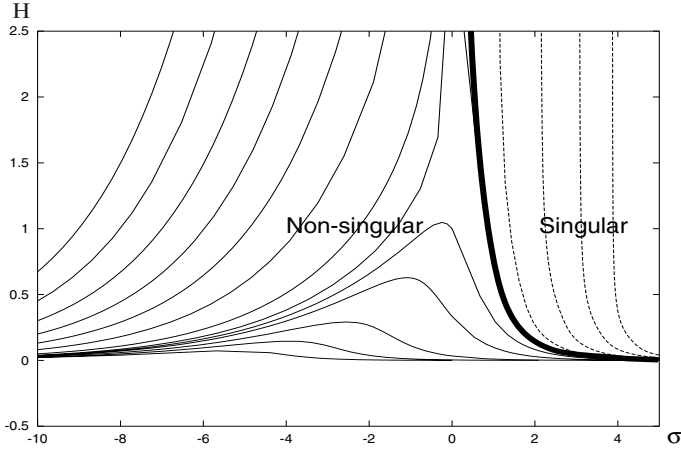


FIG. 1. The H - σ phase diagram of isotropic solutions ($\lambda = 1$, $H > 0$, $\dot{\sigma} > 0$). Time flows from left to right since $\dot{\sigma} > 0$. The non-singular solutions are plotted with solid line, and singular solutions with dotted line. The bold line is a critical solution marking the border of singular and non-singular solutions. All solution flows in $H > 0$, $\sigma < 0$ quarter plane continue smoothly to $H > 0$, $\sigma > 0$ quarter plane. In $H > 0$, $\sigma > 0$ quarter plane, however, only the flows below the critical solution continue to $\sigma < 0$ region.

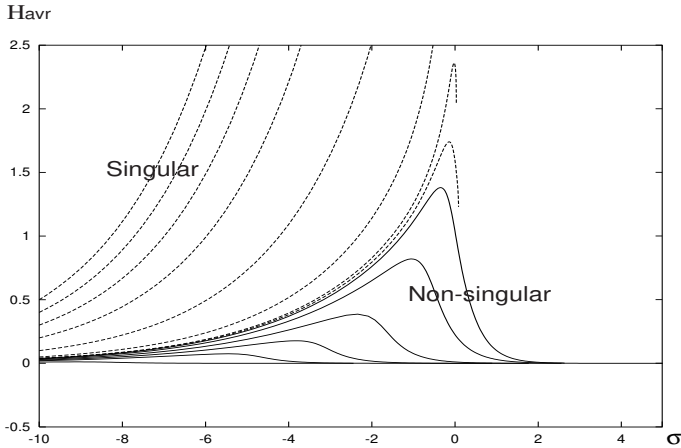
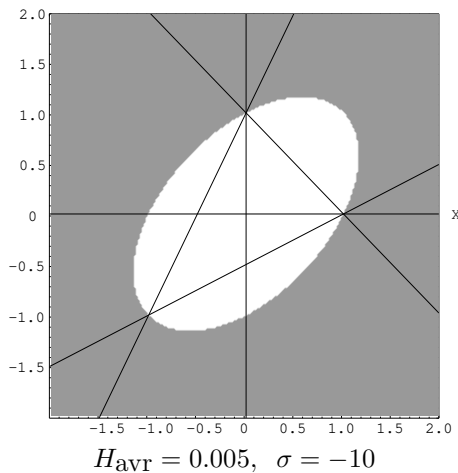
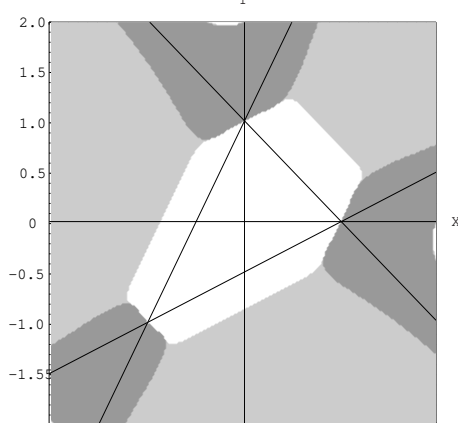


FIG. 2. The average expansion rate in the anisotropic case. The equations are solved from $\sigma = -10$, where the initial anisotropy is fixed as $X = 0.1$, $Y = 0.2$. For large initial $Havr$, there appear singularities with which the solution flows terminate suddenly, keeping $Havr$ and σ finite.

$$H_{\text{avr}} = 0.001, \sigma = -10$$



$$H_{\text{avr}} = 0.005, \sigma = -10$$



$$H_{\text{avr}} = 0.01, \sigma = -10$$

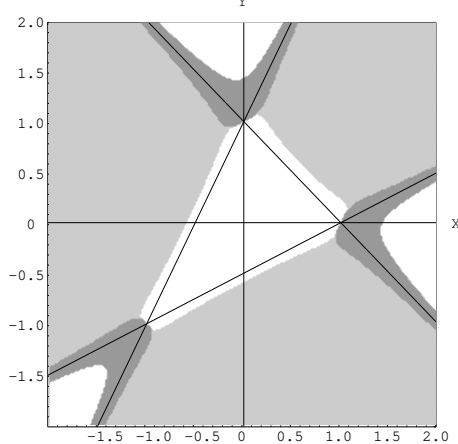


FIG. 3. Constraint and Δ on the $\sigma = -10$ section of X - Y plane. $Havr$ is 0.001, 0.005, 0.01 from above. $\Delta > 0$, $\Delta < 0$, and excluded regions are indicated by white, light-shaded, and dark-shaded areas, respectively. In the dark gray region the Hamiltonian constraint (11) is not satisfied, and Δ can not be defined. Cosmological solutions inhabit in the white and light gray regions, and those in each region are separated by singularities since p , q , r become infinite when $\Delta = 0$ (see eqns. (12),(13) and (14)).

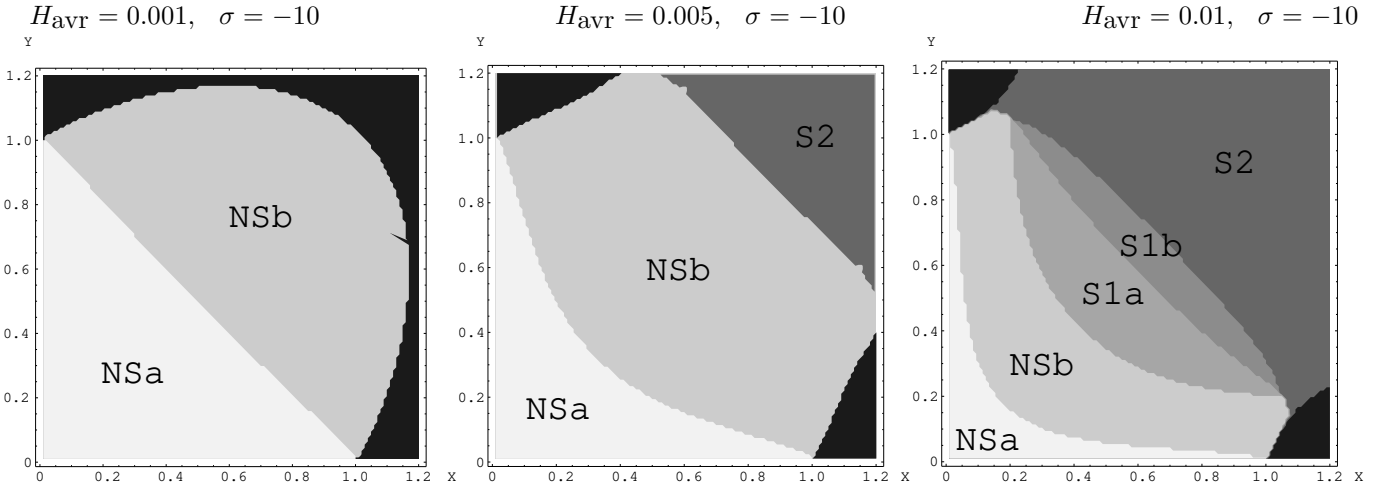


FIG. 4. Solutions through $\sigma = -10$ cross section. H_{avr} is 0.001, 0.005, 0.01 from left. NS means non-singular. NSa leads to Friedmann-type solution (expanding in all directions) and NSb leads to Kasner-type solution (expanding in two directions and shrinking in one direction) in the future asymptotic region. S1 means it leads to a singularity where $\Delta \rightarrow 0$. S1a is the solution whose behavior near such singularity is $p\dot{p} > 0, q\dot{q} > 0, r\dot{r} > 0$, while S1b behaves $p\dot{p} < 0, q\dot{q} < 0, r\dot{r} < 0$, near the singularity. S2 leads to a singularity where $\Delta \rightarrow -\infty$.

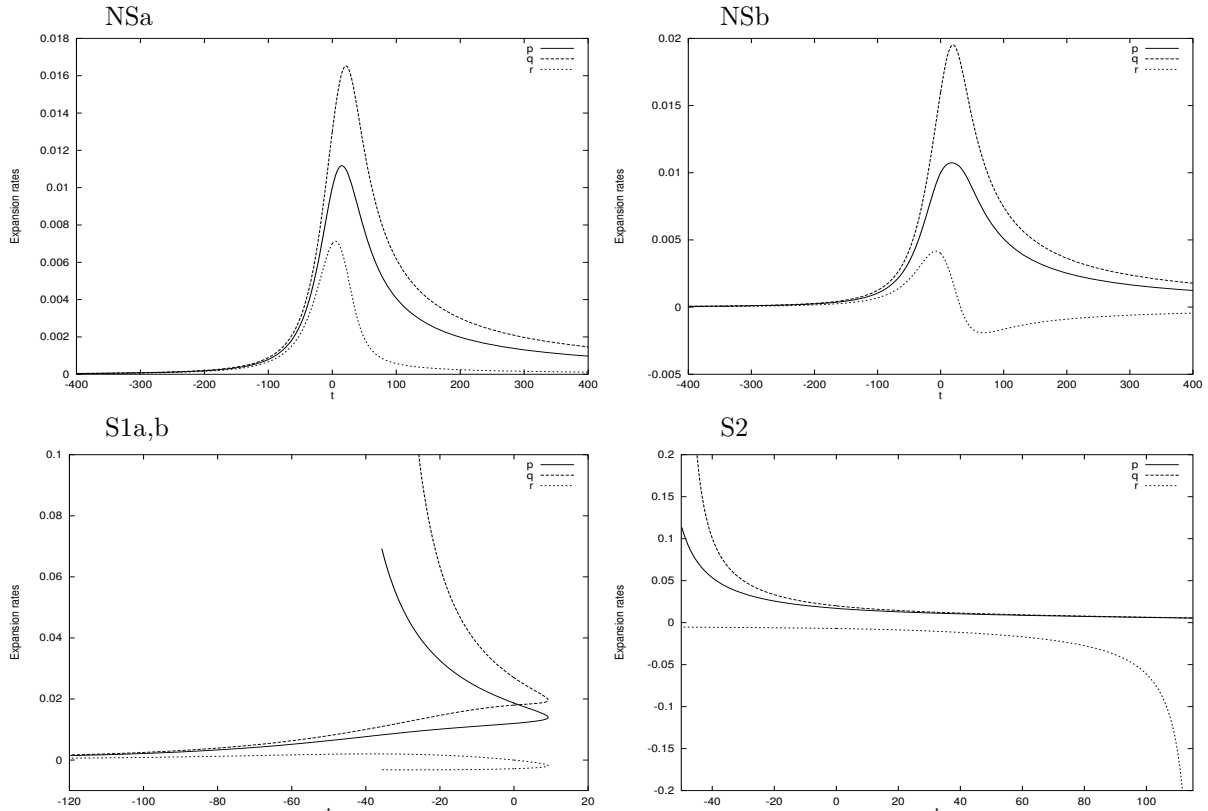
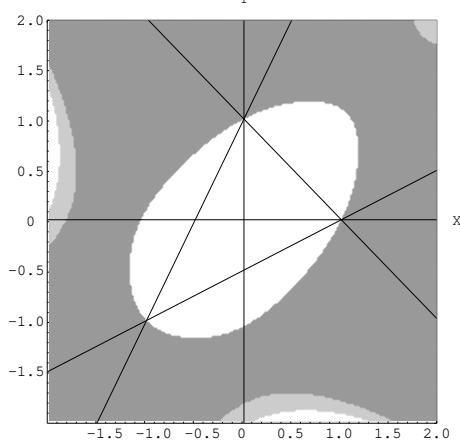
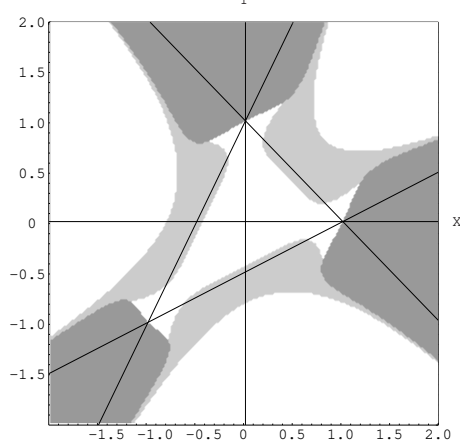


FIG. 5. Behavior of solutions appearing in the fig.4. $t = 0$ is the time when $\sigma = -10$. These are solutions through the points $(X, Y) = (0.1, 0.2), (0.2, 0.4), (0.4, 0.6)$, and $(0.8, 0.9)$, respectively in the $H_{avr} = 0.01, \sigma = -10$ plane.

$$H_{\text{avr}} = 0.1, \quad \sigma = 2.5$$



$$H_{\text{avr}} = 0.2, \quad \sigma = 2.5$$



$$H_{\text{avr}} = 0.3, \quad \sigma = 2.5$$

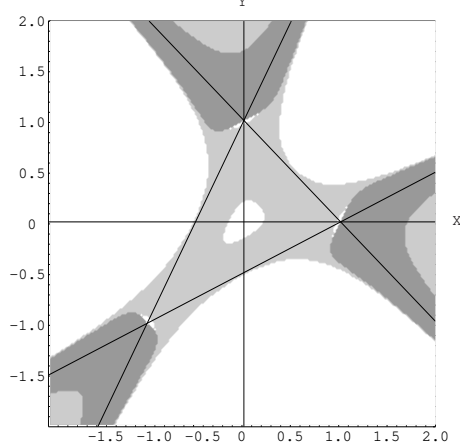


FIG. 6. Constraint and Δ on the $\sigma = 2.5$ section of X - Y plane. H_{avr} is 0.1, 0.2, 0.3 from above. $\Delta > 0$, $\Delta < 0$, and excluded regions are indicated by white, light-shaded, and dark-shaded areas, respectively.

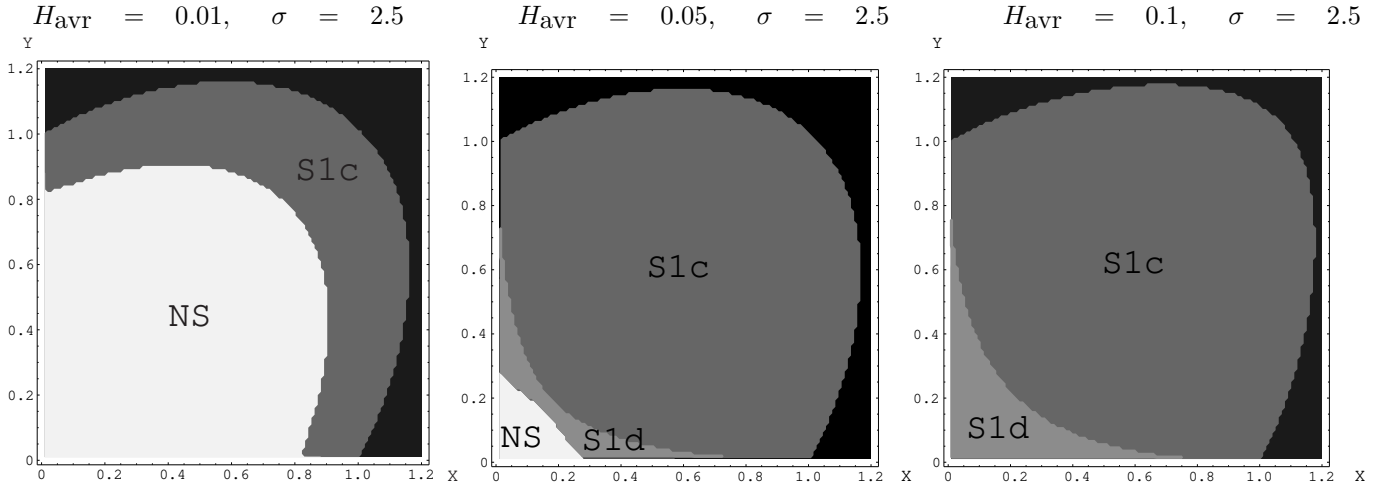


FIG. 7. Solutions through $\sigma = 2.5$ cross section. H_{avr} is 0.01, 0.05, 0.1 from left. NS means non-singular, which leads to expanding universe in the past asymptotic region. S1 means it leads to a singularity where $\Delta \rightarrow 0$. S1c is the solution whose behavior near such singularity is $p > 0, q > 0, r < 0$, while S1d behaves $p > 0, q > 0, r > 0$, near the singularity.

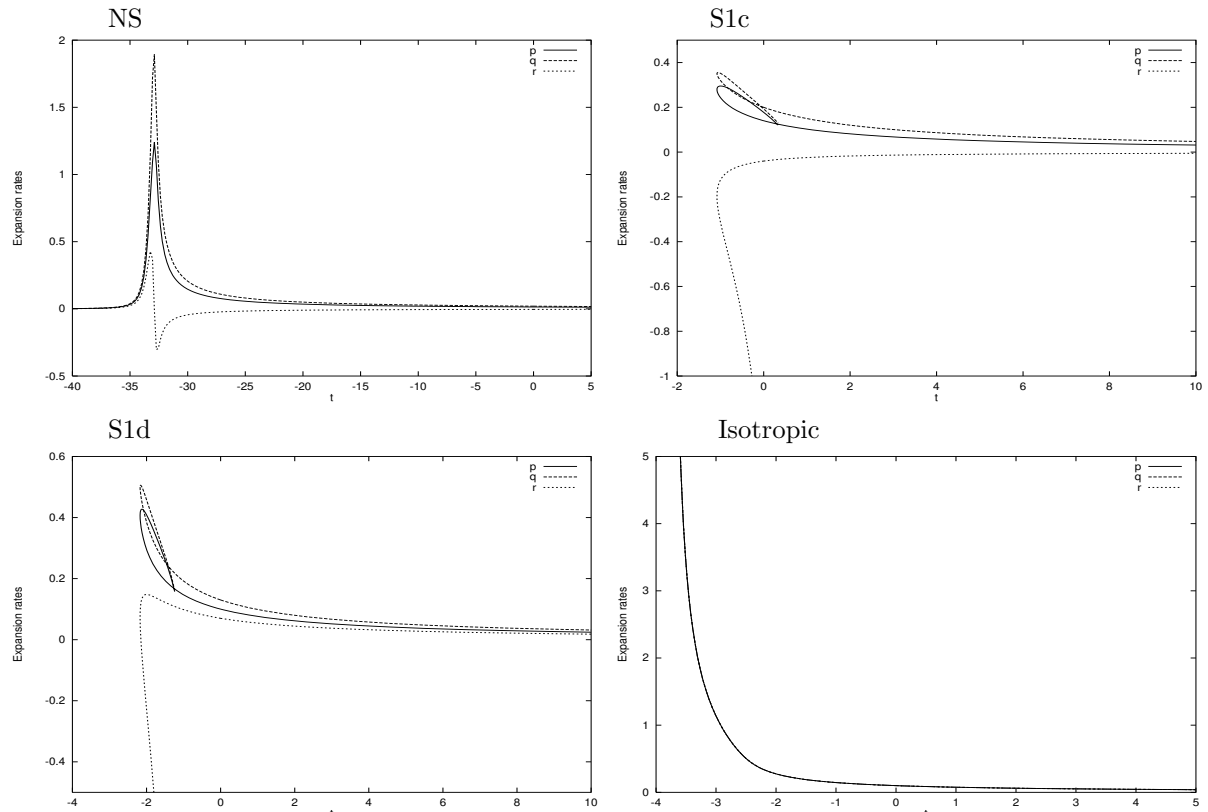


FIG. 8. Behavior of solutions appearing in the fig.7. $t = 0$ is the time when $\sigma = 2.5$. The initial values are chosen on the $\sigma = 2.5$ plane as $(H_{\text{avr}}, X, Y) = (0.01, 0.6, 0.8), (0.1, 0.6, 0.8), (0.1, 0.1, 0.2), (0.1, 0.0, 0.0)$ for NS, S1c, S1d, Isotropic example of the solution, respectively.